JOURNAL OF APPLIED POLYMER SCIENCE VOL. 14, PP. 1159–1178 (1970)

Predicting Joint Sealant Performance of Elastomers by Computer Simulation. II. Results in Simple Extension and Compression

E. H. CATSIFF, R. F. HOFFMAN, and R. T. KOWALEWSKI, *Thiokol Chemical Corporation, Chemical Division, Trenton, N. J. 08607*

Synopsis

Stress computations have been performed by a technique based on the subdivision of a body into many quasi-homogeneous elements of a material having separable time-dependent and strain-dependent mechanical properties. For several sealant materials and joint seal shapes, under simple tension and/or compression movements, results are compared to experimental data on model sealed joints. There is reasonable agreement between the predicted and experimental total stress in joint seals of all the sealants tested up to nominal joint deformations of about 20%–40%. Furthermore it has been shown that the strain distribution in the outer layer of the sealant is nonuniform and the deformed shape is nonparabolic, which disagrees with the assumptions of the joint seal analysis proposed by E. Tons. The nonparabolic deformations have been experimentally confirmed using a resin-casting technique to "freeze" the deformed joint seal to permit measurement of its shape. The computed stress and strain distributions show that the stresses are highest near the corners of the joint seal and are directed at an acute angle to the substrate, indicating that the peel strength of the sealant plays a major role in determining the overall joint strength. It has been shown how the computational technique can be applied to alternate compression and tension cycles to predict some effects of polymer stress relaxation characteristics on the stress distributions. Although the computational method has only been applied to a few representative isothermal sealed-joint systems under relatively simple loading conditions, the technique certainly has been shown to be feasible for predicting stresses within a seal over a reasonable range of nominal joint deformations. It is expected that the technique can be extended to more complex joint motions by modification of the computer programs and the input of additional data on actual joint movements. Work is in progress to extend the method in this direction and should lead to a more rational approach to sealant specifications and selection as well as improvements in joint seal designs.

INTRODUCTION

In the first paper of this series[1] a method was described for predicting the stress and strain distributions in a deformed joint seal composed of an elastomer-like material whose fundamental properties had been determined by testing simple shapes, such as ring samples and tensile strips. For the actual prediction, use was made of a digital computer program* based on

* This program is available in Fortran IV by application to the authors. We are also indebted to G. P. Anderson, W. A. Cook, and E. C. Dickson of the Wasatch Division of Thiokol Chem. Corp. for development of much of this program and for assistance in applying it to our problem.

the finite-element method of analysis of structures,[2,3] which was already available from solid rocket propellant studies. The nomenclature used in the first paper will be adopted here, too.

MODEL JOINTS STUDIED

All metal surfaces of the model joints were appropriately primed, since we wished to concentrate on the bulk response of the sealant material rather than its adhesive behavior. Some adhesive failures did occur in testing, nevertheless. The simple PbO_2-cured MT-filled polysulfide system (system A of the first paper) was chosen for initial tests of the predictive power of the computer program. Standard model joints were made up of $^1/_2$-in. square cross section of sealant and 2- or 6-in. length. It was found that joint length had a significant effect on the apparent stress–strain curve, so the latter length was subsequently standardized. Table I compares the aver-

TABLE I
Effect of Butt Joint Length on Nominal Stress–Strain Behavior[a]

	Nominal stress, psi[b]		
	2 in. long	6 in. long[c]	Computer-predicted
Extension, %			
20	43.0	62.3	—
40	67.6	90.5	89.4[e]
60	82.3	105.5	—
75	89.6	113	139.2
100	99	—	—
Ultimate extension, %	123[d]	79[f]	—
Ultimate tensile strength, nominal, psi	105[d]	114[f]	—

[a] System A, 70°F, $^1/_2 \times {}^1/_2$ in. cross section, 0.2 ipm.
[b] Nominal means referred to initial cross section of undeformed joint.
[c] Both straight bars and tee bars were used as substrates with few discernible differences.
[d] Cohesive failure.
[e] Average of three computations.
[f] Adhesive failure.

age nominal stress readings of the two joint lengths at various extensions. The Instron tester was used to extend the joints at 0.2 ipm (40%/min) at room temperature (70°F).

Quite clearly, the end effects of the 2-in. long joints permit considerable diminution of stress even at moderate extensions of the joint. At greater extensions, this end relief of stresses also permitted considerably greater joint extension before the joints broke apart. Furthermore, since this simplified sealant system was of relatively high "rubber modulus" and lacked adhesion additives, the 6-in.-long joints failed in adhesion, whereas the shorter joints failed cohesively at a slightly lower *nominal* stress level. Because of necking-down, the *actual* ultimate stress on the center section of the 2-in.-long joint seal must have been higher than that on the center section of the 6-in.-long joint seal. Adhesive stresses were probably the same in both joints at the same nominal tensile stress. Table I also lists the computer-predicted stress values at 40% and 75% extension. (In this and all computations reported, the material parameter K_2 was set at 0.49900 instead of at 0.50000 because of mathematical considerations of the computer program. This resulted in negligible computed dilatation of the joint seal.)

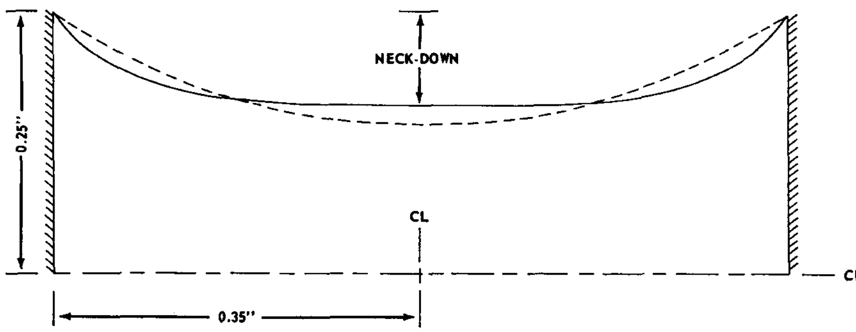

Fig. 1. Predicted cross section of $^1/_2$-in.-square model sealed butt joint extended 40%. System A extended at 40%/min. Neck-down measured at 35% elongation, 0.070–0.075 in.; (—) computer-predicted, 0.086 in.; (- - -) parabolic shape, 0.107 in.

The shape of the deformed surface of the extended joint seal was measured by clamping a test joint in the extended position, taking a negative plaster cast of the surface, and subsequently casting a hard polyurethane resin against the negative plaster cast. This cast could then be cut perpendicularly to provide a cross section for measurement.

TABLE II
Neck-down or "Curve-in" of Extended Butt-Joint Seals[a]

Extension, %	Maximum "curve-in," in.[b] Measured	Computer-predicted	Parabolic-shape[c]
35	0.070–0.075	—	0.097
40		0.086[d]	0.107
67	0.080–0.085	—	0.150
75		0.123	0.161

[a] System A, 70°F, $^1/_2 \times {}^1/_2$ in. cross section × 6 in. long, 0.2 rpm.
[b] At centerline of joint.
[c] Equation (1).
[d] Average of three computations.

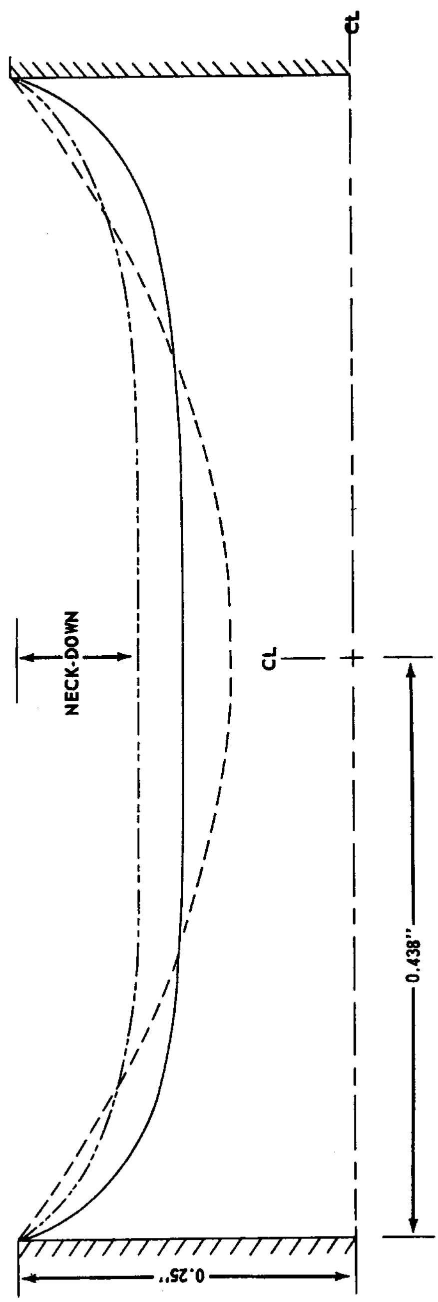

Fig. 2. Predicted cross section of $^1/_2$-in.-square model sealed butt joint extended 75%. System A extended at 40%/min: (—) computer-predicted, 0.123 in.; (- - -) parabolic shape, 0.161 in.; (- - - -) measured at 67% elongation, 0.080–0.085 in.

Such cross sections were obtained at two extensions: 35% and 67%. Our intention was to match the extensions used for computer predictions, but there were experimental difficulties. Table II compares the measured and predicted amounts of "curve-in" and also gives the curve-in predicted by the parabolic-shape formula of Tons[4]:

$$h = 0.75\, d_0\, (\epsilon/\lambda) \tag{1}$$

It is evident that the parabolic-shape formula is less accurate than the computer predictions. Particularly at the higher extension, visual inspection of the cast cross section shows clearly the flattened neck-down profile predicted by the computer. Figure 1 shows a comparison of the two shape predictions at 40%. Figure 2 shows the two predictions at 75% compared with the measured neck-down at 67%. Only the upper half is shown of the predicted joint seal shapes, while the actual profile is arbitrarily shown terminating at the same level as the predicted profiles. In actuality, the cast made at 67% was rather less precisely shaped, particularly at the edges, than the drawing indicates, so the actual neck-down could well be somewhat larger than 0.085 in.

The kind of stress distribution prediction possible is shown in Figure 3. This shows the quarter-section of the system A joint seal at 1.0 min while being stretched at 40%/min. Table III gives more details of the computer predictions at 40% and 75%. From the angle at which the maximum tensile stress is applied in the corner of the joint seal, it is apparent that strong peeling forces will come into play even in a straight pull on a simple butt joint. This suggests that 180° adhesive peel tests are of considerable importance in specifying joint-sealant practice, even for butt joints, and

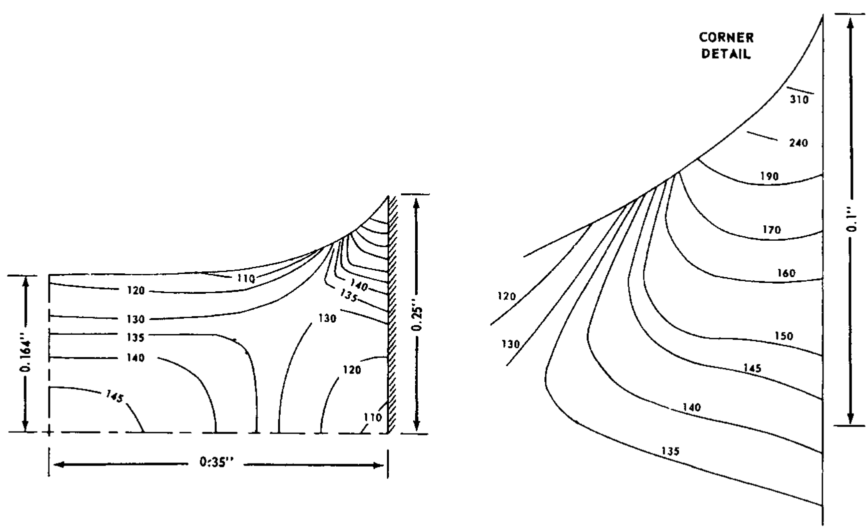

Fig. 3. Predicted maximum principal stress distribution in quarter-section of sealed butt joint of Figure 1. Numbers on contour lines are stresses in psi.

TABLE III
Predicted Behavior of Butt-Joint Seals in Extension[a]

Job no.	200568[h] 250668 060369-3	120968	061268-3
Joint size, in.[aa] and shape	0.5 × 0.5 × 6 square	0.5 × 0.5 × 6 square	2 × 1 × 5 rectangular
Extension, %	40	75	20
Extension rate, %/min	40	40	20
Measured tensile stress, psi nominal[b]	90.5	113	78.0[k]
Centerline tensile stress, psi nominal[b]	89.4[q]	139.2	70.0
Maximum "curve-in," in.[c]	0.086[q]	0.123	0.231
Maximum tensile stress, psi[d]	350[r]	655	311[g]
Angle to substrate[e]	33°[r]	26°	34°
No. of iterations	9[m] 9[n] 7[p]	7	7
Relative mean error[f]	0.00174[m] 0.00161[n] 0.00924[p]	0.00143	0.00934

[a] System A, 70°F, crosshead speed 0.2 ipm. All predictions at next-to-last iteration except where noted.
[aa] Depth × width × length.
[b] Referred to original cross section; "centerline" refers to location of summed stress elements.
[c] Displacement downward at centerline.
[d] In extreme corner of joint; original position was 0.005 in. down from edge and 0.005 in. from wall except where noted.
[e] Of maximum tensile stress; 0° is parallel to wall.
[f] For last iteration.
[g] Original position was 0.010 in. down from edge and 0.010 in. from wall.
[h] Three different meshes have been used for this calculation.
[k] One specimen, see text.
[m] Job No. 200568, 20 × 12 uniform mesh. A 20 × 20 mesh has 20 rows of 20 nodes each, defining 361 elements in the quarter-section. In the nonuniform mesh, the elements closest to the substrate wall, and to the free surface of the joint seal, were considerably reduced in size to provide detail in these regions comparable to that of the 20 × 20 uniform mesh.
[n] Job No. 250668, 12 × 12 uniform mesh.
[p] Job No. 060369-3, 12 × 12 nonuniform mesh, looser convergence required.
[q] Average of three calculations.
[r] Job No. 060369-3 only; other jobs were not detailed enough in corner, but are in agreement.

strongly validates the inclusion of these tests in Interim Federal Specifications.[5a]

Some additional work was attempted with system A, in a joint seal of different cross section. In this joint seal, 1 in. wide by 2 in. deep, even greater deviation from the parabolic-curve assumption was expected.[4] A single 5-in.-long test joint was prepared and stretched on the Instron

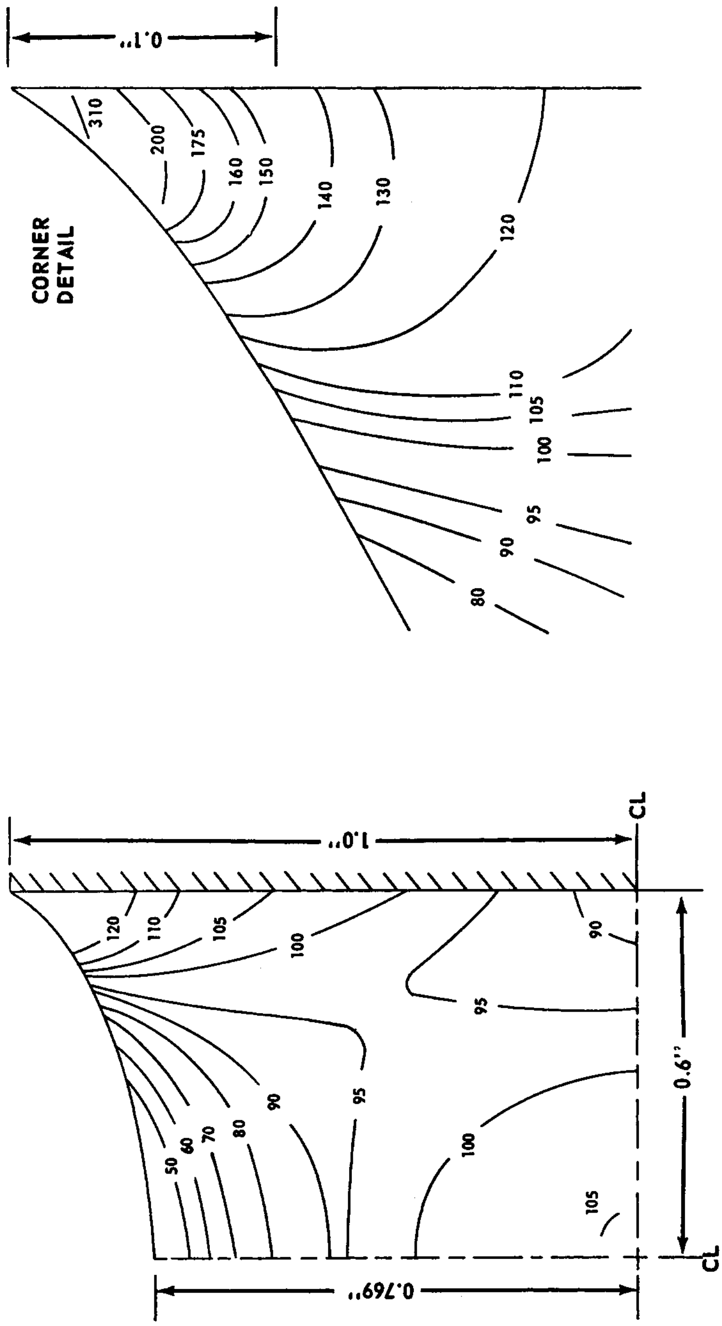

Fig. 4. Predicted maximum principal stress distribution in quarter-section of "deep" model sealed butt joint. Original dimensions: 1 in wide × 2 in. deep. System A extended 20% at 20%/min.

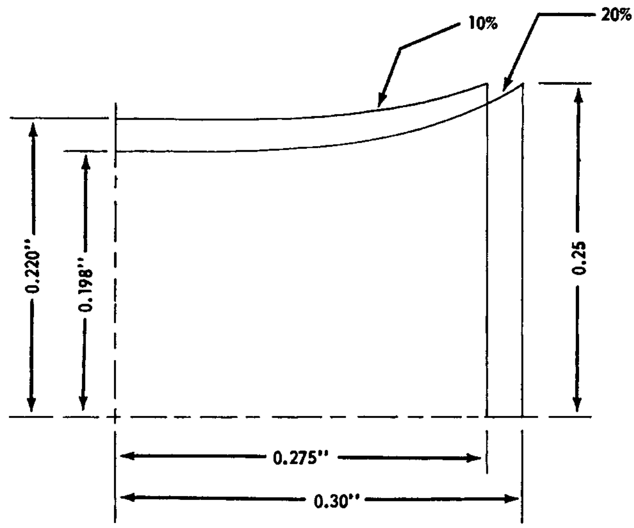

Fig. 5. Predicted deformation of quarter-section of 1/2-in.-square model sealed butt joint extended 10% and 20%. System B (time-independent behavior).

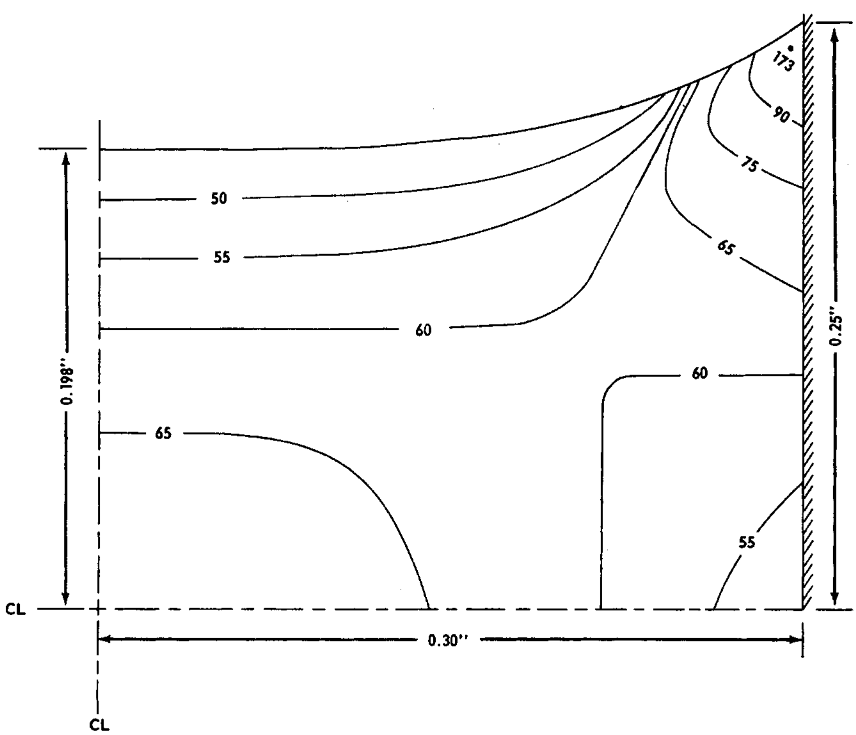

Fig. 6. Predicted maximum principal stress distribution in quarter-section of sealed butt joint of Figure 5 extended 20%.

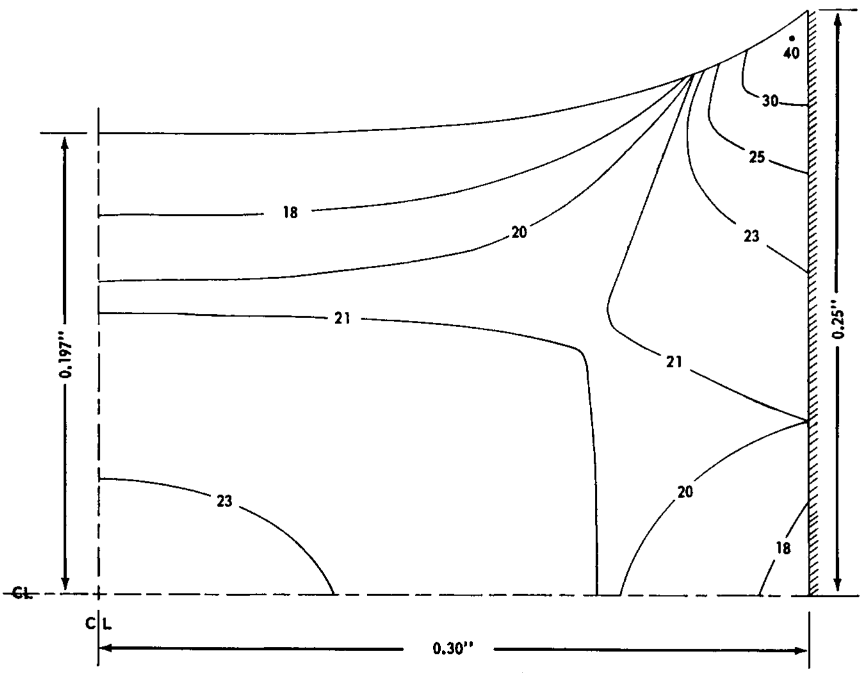

Fig. 7. Predicted maximum principal stress distribution in quarter-section of $^1/_2$-in.-square model sealed butt joint extended 20%. System D extended 40%/min.

tester at 0.2 ipm (20%/min in this case). Testing proved to be difficult because of slippage in the testing machine. After several false starts, a stress–strain curve up to 25% elongation was obtained before slippage. Some later extensions of the same specimen that were partially successful showed 15–20% lower forces at 20% extension, suggestive of a "Mullins effect."[6] The one run considered probably valid for unstretched material was compared with the computed result at 20% extension; the latter is shown in Figure 4. Details of the computed results are given in the last column of Table III.

Having found that the simplified system A material's behavior could be predicted in simple seals, we proceeded to study test joints of other systems. System B, a silicone sealant, had shown no time dependence in the ring-sample test. When $^1/_2 \times {}^1/_2 \times 6$ in. test joints were pulled at 40%/min, adhesive failure occurred in all cases, at extensions between 70% and 140%. Three joints were pulled at 400%/min (2 ipm); all failed in adhesion at 40% to 80% extension, i.e., at lower stresses than in the slow speed tests. At 40% extension, stress was of about the same magnitude as in the slow speed tests (as would be expected if material properties were time independent), but the recorded curves were unsuitable for detailed analysis. Some sort of time-dependent behavior of the primer may be adduced here. (A test joint which slipped repeatedly in the testing machine, and so was retested, showed a "Mullins effect." Since this commercial sealant apparently contained filler, this is not too surprising.)

Computer-predicted shapes of the test joint quarter-sections at 10% and 20% extension are shown in Figure 5; the maximum local stress isodynics at 20% extension are shown in Figure 6. Table IV gives further details of the computer predictions, including comparisons with measured nominal stress results.

TABLE IV
Butt-Joint Seal Behavior of Commercial Sealants[a]

Job no.	291068	281068	261268-1	060369-1
Material system	B	B	D	E
Extension, %	10	20	20	20
Measured tensile stress, psi nominal[b]	21.5	36	14.1	12.1
Centerline tensile stress, psi nominal[b]	24.9	48.3	16.6	15.1
"Maximum "curve-in," in.[c]	0.0291	0.0525	0.0525	0.0526
Maximum tensile stress, psi[d]	82	173	59	54
Angle to substrate[e]	49°	42°	42°	42°
Relative mean error[f]	0.00008	0.00020	0.00021	0.00029
No. of iterations	7	7	7	7

[a] 70°F, $^1/_2 \times {^1/_2} \times 6$ in., 40%/min. All predictions at next-to-last iteration except where noted.

[b] Referred to original cross section; "centerline" refers to location of summed stress elements.

[c] Displacement downward at centerline.

[d] In extreme corner of joint; original position was 0.005 in. down from adhered edge and 0.005 in. from wall.

[e] Of maximum tensile stress; 0° is parallel to wall.

[f] For last iteration.

Also shown in Table IV are computer predictions and measured nomina stress results of two other commercial sealants (systems D and E) in $^1/_2 \times {^1/_2} \times 6$-in. test joints at 20% extension (at 40%/min). These latter two are much softer materials than systems A and B, so that much lower stress levels were attained. The detailed stress distributions at 20% extension of the test joint of system D is shown in Figure 7. It was noted that the stress–strain and K_1 isochrones of systems D and E were quite similar; this is reflected in both the computed and the measured values of Table IV. It may be inferred that these two commercial sealants have been formulated to give very similar mechanical behavior, at least when the sealed joints are still fairly fresh, despite the obvious chemical dissimilarity of their polymeric constituents.

Although the material property parameters (i.e., the K_1 isochrones) were determined from constant strain rate tests in simple extension, there is no obvious reason why they should not be usable in constant strain rate testing in simple compression. To see if this was so, $^1/_2$-in.-square test joints of system A were compressed at 40%/min. When two 2-in.-long joints were compressed, the end effects were significant and quite obvious: the sealant material squeezed out the ends and was sheared through by the metal backing plates. Six-in.-long joints which were filled flush to the surface of the metal backing bars gave higher nominal stresses with much less end effect. A plaster-cast negative and cast polyurethane positive replica was obtained of such a joint clamped at 25% compression. It clearly showed not only the "bulge-up" that would be expected, but also an overhang of the lip of the joint, as shown in Figure 8.

Computer prediction of this result proved exceedingly difficult. This was not because of inapplicability of the material property parameters, but because the bulging up of some of the finite elements led to a theoretically unstable condition, akin to the buckling of a thin strut under a compressive load. Consequently the computed displacements began to wander and the average fractional displacement ("mean error" in program terminology) remained fairly large and eventually diverged. By forcing termination even though the normal convergence criterion had not been met, it was

TABLE V
Compression of Butt Joint[a]

Job no.	101068[c]	241068-3[d]	211068[c]	231068	161068
Compression, %	24.2[c]	25.0[d]	24.2[c]	25.0	10
Type	free bulge	free bulge	high wall[g]	high wall[h]	free surface
Measured compressive stress, psi nominal[aa]	—	130	—	—	53
Centerline compr. stress, psi nominal[aa]	137.4	141.8	139.4	141.2	37.2
Measured "bulge" upward[b]	—	0.11–0.12	—	—	—
Maximum "bulge" upward[b]	0.0963	0.1011	0.0973	0.1024	0.0351
Measured side bulge, in.	—	0.005	—	—	—
Maximum side bulge, in.	0.0089	0.0099	—	—	none
Relative mean error[e]	0.03969[j]	0.05609[j]	0.03807	0.00176	0.01189
No. of iterations	6[c]	5[d]	6[c]	8	7

[a] System A, 70°F, $^1/_2 \times ^1/_2 \times 6$ in., 0.2 ipm. All predictions at next-to-last iteration, except where noted.
[aa] Referred to original cross section.
[b] At centerline.
[c] Forced termination with stress calculation after 5th iteration.
[d] Terminated with stress calculation after 4th iteration; incipient buckling.
[e] For last iteration, except where noted.
[g] Pressed to wall 0.033 in. above corner.
[h] Pressed to wall 0.028 in. above corner.
[i] On next to last iteration; last iteration had rise in relative mean error.

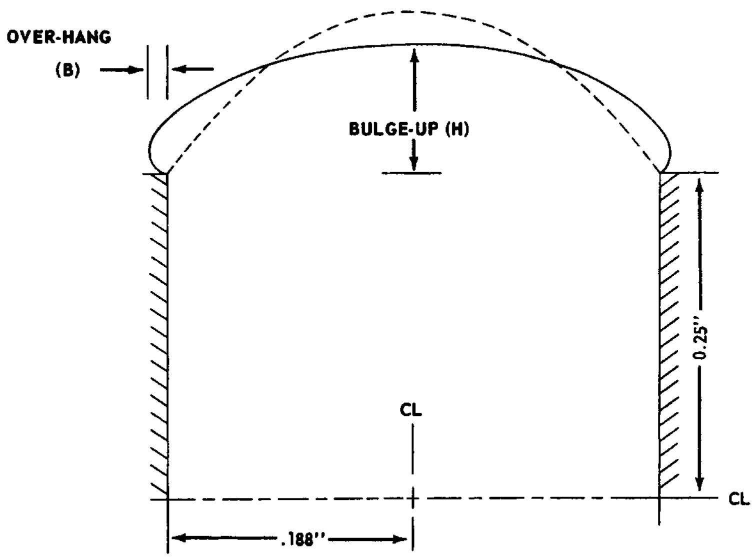

	BULGE-UP (H)	OVER-HANG (B)
——— COMPUTER PREDICTION:	0.101"	0.010"
------ PARABOLIC SHAPE:	0.125"	NOT PREDICTED BY ASSUMPTION
MEASURED:	0.110"	0.005"

Fig. 8. Predicted half-section of $^{1}/_{2}$-in.-square model sealed butt joint compressed 25% without confinement. System A compressed 40%/min.

possible to get not only a predicted shape but even a reasonable pattern of stress distributions along the joint centerline, so that a centerline compressive stress could be predicted. These results are given in Table V. Calculated stress distribution throughout the joint seal was extremely erratic, however, particularly near the corner where the overhang existed.

Also given in Table V are results obtained when the input restrictions on node movement during compression were modified to require the free surface to remain within the region specified by extending the wall surfaces up beyond the fill level of the sealant. With the options available in the existing program, this required arbitrarily specifying how much of the free surface would actually be forced into contact with the "high wall." Two slightly different specifications were prescribed; both gave nearly the same stress summation along the centerline, so the computation based on the lesser amount of constrained surface was chosen and is shown in Figure 9. (If the chosen constraint were too little, the "buckling" problem of Figure 8 would have resulted; it too much, a *tensile* strain would be imposed on the elements lying above the original fill line. The sharp onset of buckling dictates the specification of the minimum constraint which avoids such difficulty.) Finally, in Table V, the result is given of a computed 10%

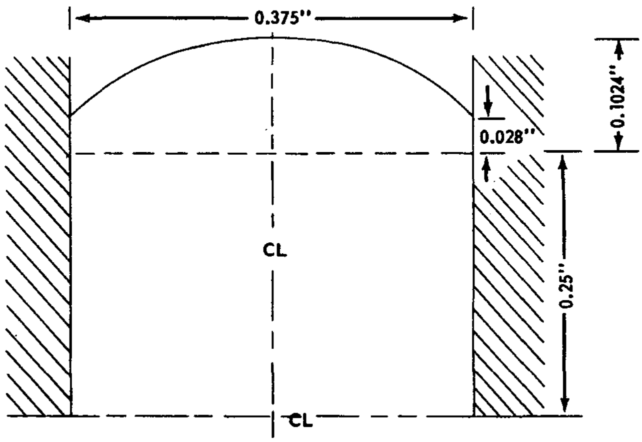

Fig. 9. Predicted half-section of sealed butt joint of Figure 8 compressed 25%, confined between walls.

compression of the test joint; in this case no overhang and no buckling problem were found.

At 10% compression, the predicted compressive stress was substantially too low. This implies that the K_1 values used (the short-time values) were too low, perhaps because of the difficulty of measuring stress and strain in the ring samples at the very start of the deformation test.

At 25% compression, all the cases shown predicted nearly the same "centerline" compressive stress, which is 5–10% too high. This is taken to be a reasonable confirmation of the validity of using extension test isochrones in a compressive situation.

COMPUTER SIMULATION OF MORE COMPLEX SITUATIONS

While it is intellectually gratifying to predict the behavior of simple joint seals under simple applied loads, the underlying purpose of this work is to use the same mathematical apparatus to predict the behavior of more complex situations. The available computer programs do not incorporate the sophisticated options that could be used for many practical conditions. However, even within the limits of immediate availability, some fairly complex configurations may be examined.

In the stretching of a square or rectangular butt joint, the region of greatest local stress (most of which exerts a peeling force) is found in the extreme corner of the joint seal. This appears to result from the need of the joint seal material to neck down when it is stretched at essentially constant volume. It might naively be supposed that a filled surface which had been tooled so that it departed from the substrate wall at an obtuse angle (i.e., the angle defined by the free surface and the coated part of the wall is greater than 90°) would provide more material to undergo neckdown. Thus it would give a stretched profile in which the local tensile

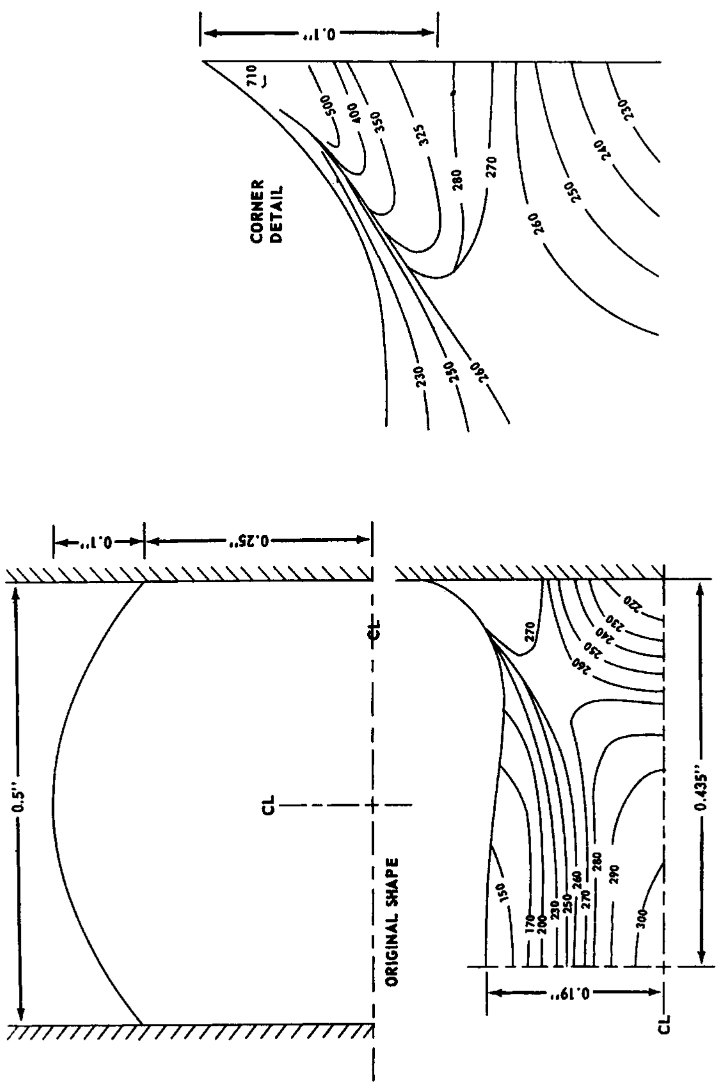

Fig. 10. Predicted deformation and maximum principal stress distribution in quarter-section of arbitrarily shaped butt joint seal extended 75%. System A extended 40% min^{-1}.

TABLE VI
Predicted Behavior of a Compressed Butt Joint after Relaxation[a]

Job no.	010469-1	111168	120968	See Table III[h]
Joint size, in.,[m] and shape	0.375 × 0.556 bulged to 0.705 in. deep[j]	0.5 × 0.5 bulged to 0.7 in. deep[k]	0.5 × 0.5 square	0.5 × 0.5 square
Extension, %[aa,g]	67	74	75	40
Extension rate, %/min[aa,g]	53	39.5	40	40
Centerline tensile stress, psi nominal[b]	176.3	174.2	139.2	89.4[q]
Maximum "curve-in," in.[c]	0.156	0.160	0.123	0.086[q]
Maximum tensile stress, psi[d]	1375[s]	711[t]	550	290[r]
Angle to substrate[e]	22°	27°	26°	33°[r]
No. of iterations	8	7	7	See Table III
Relative mean error[f]	0.00575	0.00897	0.00143	See Table III

[a] System A, 70°F, crosshead speed 0.2 ipm. All predictions at next-to-last iteration except where noted.

[aa] Referred to unstretched width.

[b] Referred to 0.5-in. depth adhering to wall; "centerline" refers to location of summed stress elements.

[c] Displacement downward at centerline.

[d] In extreme corner of joint; original position was 0.010 in. down from adhered edge and 0.005 in. from wall except where noted.

[e] Of maximum tensile stress; 0° is parallel to wall.

[f] For last iteration.

[g] Extension actually used in computation of stresses.

[h] Three different meshes have been used for this calculation.

[j] Compressed from 0.5 × 0.5 × ∞ at 0.2 ipm and fully stress relaxed.

[k] Arbitrarily bulged profile.

[m] Width × depth at wall; all joints are "infinitely long."

[q] Average of three calculations.

[r] Average of two calculations; third job was not detailed enough in corner, but is in agreement.

[s] Original position in joint *before* compression was 0.010 in. down from adhered edge and 0.005 in. from wall; in compressed, fully relaxed joint, this material point was 0.005 in. down from adhered edge and 0.003 in. from wall.

[t] Original position was 0.0106 in. down from adhered edge and 0.0106 in. from wall; mesh was not detailed enough in corner.

stresses were directed more nearly perpendicular to the wall and were more evenly shared by the material used. It might even be supposed that such a shape would permit use of material having poorer peel-adhesion strength. Such a shape is shown in Figure 10. It has been pointed out that a bead shape commonly found in joints has just such a convex profile on its inaccessible underside.[7]

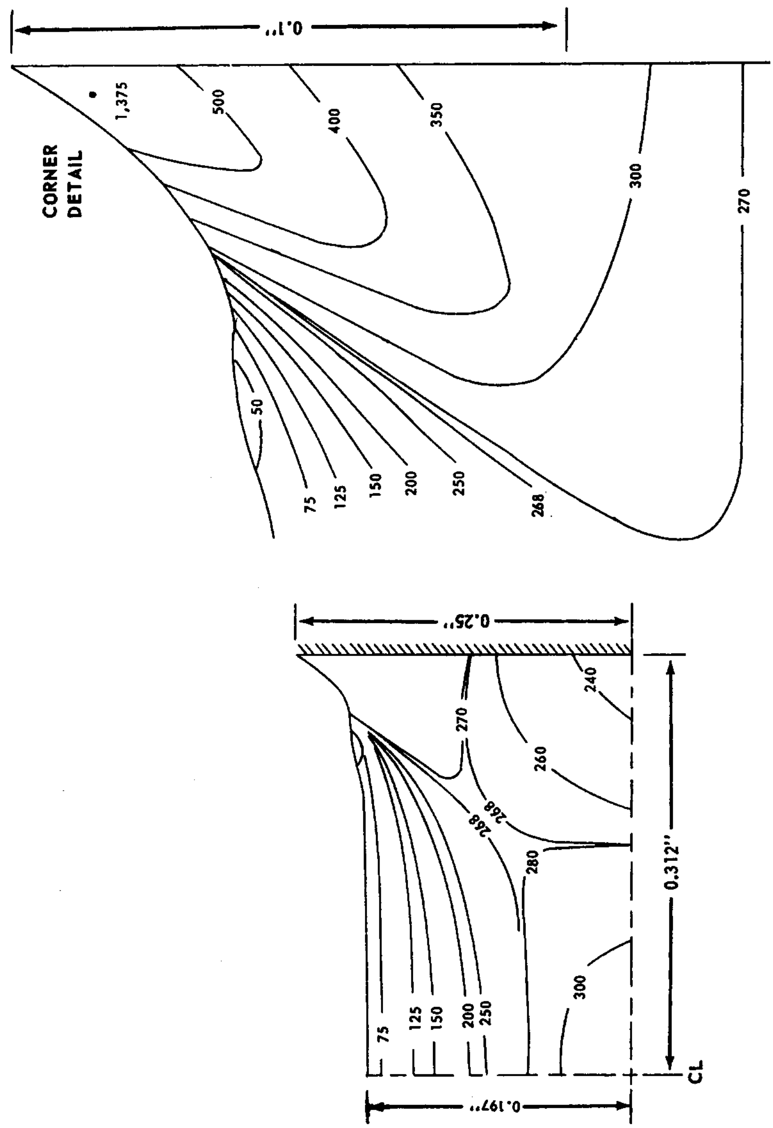

Fig. 11. Predicted deformation and maximum principal stress distribution in quarter-section of butt joint seal of Figure 9. Original $^{1}/_{2}$-in.-square cross section compressed 25% and fully stress relaxed, then reextended to net 25% extension at 0.2 ipm.

The computer run was made using the material constants of system A at 1.875 min, for an input extension of 75%. (Because of the "creeping-up" process used in the program and a fairly loose convergence requirement, the job terminated at 74% extension, certainly within the required accuracy.) The stretched shape is shown in Figure 10, with the computed stress distributions. Table VI gives more details of the computation. A large part of the cross section is a region where computed local maximum stresses varied erratically, indicating possible mathematical-mechanical instability in the solution of the problem. The isodynics in this region are somewhat speculative. Figure 10 shows that the bulged profile results in generally high local stresses throughout the stretched joint, including high peel forces in the corner, but that the added material in the bulge is less stressed. One consequence of this is that the local maximum forces along the top surface must change drastically in a very small area near the corner. Table VI also includes the results of the computer prediction of the square joint at 75% extension from Table III. Comparison clearly shows *intensification* of stresses in the critical peeling region near the joint seal corner. This confirms Garden's conclusions[7] about the effect of sealant bead shape on performance.

After this computation had been performed, it was noted that the original bulged profile somewhat resembled that produced by compression of a $^1/_2$-in.-square joint seal confined between parallel plates, as shown in Figure 9. If the material of the joint seal is able to relax stress chemorheologically, then, to a first approximation, a subsequent stretching of the fully relaxed joint seal should be calculable, using the material properties parameters already known for the original sealant material. (If the joint seal material undergoes changes which affect its properties, the parameters must be determined on appropriately aged ring samples.) In essence, then, Figure 10 indicates the behavior of a joint seal of a chemorheologically stress-relaxing material in a butt joint that undergoes infrequent but rapid reversal from compression to extension.

As a direct test of the behavior to be expected from a fully stress-relaxed compressed joint seal, this calculation was perhaps inadequate for several reasons:

(1) The bulged profile was arbitrarily chosen and did not necessarily correspond to the profile of a compressed square joint seal.

(2) The depth-to-width ratio of the joint seal was different from that of a compressed square joint seal. This ratio is of great importance in determining joint seal behavior.[4,7]

(3) The entire wall-contact area of the sealant was assumed to be perfectly adherent to the wall. As shown in Figure 9, a 25% compressed square joint seal has considerable nonadherent material in contact with the wall. (To some extent, this may compensate for the greater depth-to-width ratio of the compressed square joint seal.) It may be postulated that, during the process of chemorheologic stress relaxation, the additional contact area becomes fully adherent, resulting in a situation resembling job

no. 111168. However, it was of interest to calculate joint seal behavior in the absence of such adhesion.

Also, the joint extension chosen was 75% in the prior case, at 40%/min. A compression–extension cycle of considerable interest (because it is given in Interim Federal Specifications[5b]) is 25% compression followed by 25% extension (based on the original joint dimension). This is a 67% extension of the compressed joint and, at the same absolute crosshead speed, corresponds to 53%/min.

A computation was performed using the material properties of system A at 70°F and 1.25 min extension time, with the joint dimensions of Figure 9 extended at 0.2 ipm. Figure 11 shows the calculated shape and stress distribution pattern, while Table VI gives more details of the computation.

The most striking features of the reextended joint are the wrinkle on the surface of the stretched joint seal and the very high stress concentration and peeling forces in the corner. The wrinkle is of the same dimensions as the mesh size of the finite-element program in the corner, so it is rather poorly resolved; but its existence corresponds to observations of cyclically flexed joints, so that it may well be a real phenomenon.

The calculated stress in the extreme corner of the joint seal is about three times as high as would be calculated if the original joint had simply been stretched 67%, and is probably six to eight times the calculated stress if the original joint were simply stretched 25%; i.e., if there had been no stress relaxation in the compressed joint seal, the material in that case being fully elastic and the subsequent extension regarded as starting from zero when the joint width again reached 0.500 in.

This computation shows that this compression–extension cycle is far more rigorous when applied to a chemorheologically stress-relaxing sealant (particularly one of abnormally high modulus, such as system A) than when applied to a nonrelaxing material. On the other hand, a compression–extension cycle which provided small increments of deformation, with periods of possible stress relaxation between increments, would probably prove to be a very mild test for a chemorheologically stress-relaxing material, even if the total deformation were considerably greater than ±25%. For a nonrelaxing material, only the overall amount of deformation would be significant; if this were large, no matter how slow the rate of attainment, a severe requirement would be imposed.

Thus, in drawing up performance specifications, it is necessary to match the specifications to the job at hand; overspecifying the requirements may result in choosing a material that would be unsatisfactory in use *precisely because* it is designed to pass a fundamentally irrelevant specification.

The results of this computation also cast some light on the results of job no. 111168. Because the mesh size of this job was chosen rather large and uniform, corner detail was inadequate. Thus, even the high forces shown there were a serious underestimate of what could be expected from an originally bulged profile. Also, the wrinkle in Figure 11 appears to result from the nonadhered corner of the joint seal in Figure 9; it could not appear in job no. 111168. However, Figure 10 does show the stretched surface of the latter joint seal to be doubly curved. The question of whether the material in a confined, compressed joint would adhere to the wall above the original filling line remains open. Intuitively, partial adhesion might be expected. The available computer program is not sophisticated enough to handle such a situation.

CONCLUSIONS

The examples presented show that the finite-element approach can be used for computer simulation of joint seal behavior and that time-dependent material properties can be incorporated. For moderate deformations of long simple joints, predictions based on a modulus-like parameter at constant volume in plane strain appear to be reasonably accurate. Similar predictions can be made for stresses and strains in joint seals of various other configurations and loading conditions, providing that an appropriate series of stress–strain curves, on geometrically simple samples, can be determined in the laboratory. It is not necessary, and is even fallacious, to assume in advance either an analytic description of the shape of the deformed joint seal or a uniform stress or strain distribution.

Further utility of the method includes the possibility of comparing predicted behavior of different materials, including changes in formulation, on the basis of relatively few laboratory tests and a small amount of verification testing. Comparison of joint design factors can also be made, particularly since considerable detail of the stress and strain distributions can be obtained, so that particular weak spots may be pinpointed.

Study of actual joint failures is an important corollary of this approach. It should be possible, in many cases, to relate regions of stress concentration or high strain-energy density to initiation of failure. The ingenuity of designers and formulators can then be turned to avoidance of these situations, with computer simulation of proposed solutions as a valuable aid to shorter development time.

To make this possible, further development of the simulation procedure is desirable. The results of temperature cycling (diurnal and annual) and the imposition of more complex movements need to be considered. Not all of the options in the available computer program have yet been explored, and certain additional features can be readily added to increase the power of this method. Design of still more powerful programs and planning of more convenient methods of using computers are other future developments that may assist the joint seal designer. A better understanding of the behavior of sealants in joints is clearly possible and desirable. More rational ways to specify sealants and sealant usage would be a valuable result of such understanding.

References

1. E. H. Catsiff, R. F. Hoffman, and R. T. Kowalewski, *J. Appl. Polym. Sci.*, **14**, 143 (1970).

2. L. R. Herrmann, *A.I.A.A.J.*, **3**, 1896 (1965).

3. L. R. Herrmann, Bulletin of the 4th Meeting, ICRPG, Working Group on Mechanical Behavior, Vol. 1, Nov. 1965, p. 405.

4. E. Tons, *A Theoretical Approach to Design of a Road Joint Seal*, Highway Research Board, Bulletin 229, January 1959.

5. Interim Federal Specification TT-S-00230b(COM-NBS), Sept. 25, 1968; *ibid.*, TT-S-00227D(COM-NBS), Oct. 23, 1968. (a) Sections 4, 3, 10; (b) Section 4, 3, 9.

6. J. A. C. Harwood, L. Mullins, and A. R. Payne, *J. Appl. Polym. Sci.*, **9**, 3011 (1965).

7. G. K. Garden, Use of Sealants, *Canadian Building Digest*, CBD96-1, AD 675 701, Dec. 1967.

Received October 24, 1969
Revised January 16, 1970